Brain Pathology 8: 19-27(1998)

RESEARCH ARTICLE

Identification of the End Stage of Scrapie Using Infected Neural Grafts

Sebastian Brandner[1], Stefan Isenmann[2], Guido Kühne[3], and Adriano Aguzzi[1]

[1] Institute of Neuropathology, University Hospital, CH-8091 Zürich
[2] Department of Neurology, University of Tübingen, D 72076 Tübingen
[3] Paul Scherrer Institute, CH 5234 Villigen

Although the formal pathogenesis of spongiform encephalopathies has been described in detail, it is not known whether the infectious agent targets primarily neurons, glial cells, or both. To address this question, we have transplanted transgenic embryonic neural tissue overexpressing PrP^C into the forebrain of *Prnp* -knockout mice, and infected it with scrapie prions. After infection, grafts developed severe spongiform encephalopathy. As the infected hosts were not clinically affected, we were able to prolong the experiment and to assess changes in the graft over periods of time, which vastly exceeded the normal life span of scrapie-infected mice. Sequential contrast-enhanced magnetic resonance imaging (MRI) revealed progressive impairment of blood-brain barrier properties in infected grafts. However, loss of astrocytes was not observed. Subtotal neuronal loss occurred during the progression of the disease in the grafts, reactive astrocytes persisted until the terminal stage of disease. We conclude that scrapie encephalopathy primarily leads to neuronal death, while degeneration of astrocytes does not occur. Functional impairment of the blood-brain barrier suggests involvement of astrocytes and endothelial cells in the pathological process.

Introduction

Transmissible spongiform encephalopathies, or prion diseases, show typical histopathological features in the central nervous system. The most prominent findings are vacuolization and reactive astrogliosis (11). Concurrent neuronal loss is frequently observed (22), but in some instances this feature is not obvious and only detectable after detailed morphometric analysis or in specific experimental systems (21, 25). For instance, prominent neuronal loss in the hippocampus is encountered e.g. in LM mice and in C57BLxVM mice after inoculation with the scrapie strain ME7 while scrapie strain 22A does not cause detectable alterations in the hippocampus of C57BLxVM mice (24), retinal neuronal degeneration has been observed after scrapie infection of hamster and of certain mouse strains (8, 9, 15). However, hippocampus and retina contain highly ordered neuronal structures, and it is very difficult to assess quantitative changes in cell populations in areas lacking the latter, such as the cerebral cortex.

Recent transgenetic studies revealed that mice expressing increased amounts of the normal cellular prion protein (designated PrP^C) in their brain develop scrapie with a shortened incubation time after intracerebral scrapie infection (60 days) as opposed to 160 days in wild type mice. Despite this more severe clinical course of the disease, the brain of these mice displays remarkably little gliosis, no significant neuronal loss, and very little accumulation of abnormal prion protein (PrP^{Sc}) (3, 14). In contrast, hemizygous mice carrying only one functional copy of the *Prnp* gene, and expressing approx. 50% of the PrP^C found in wild type mice, enjoy a relatively mild clinical course despite severe gliosis and more prominent neuronal loss (5).

A straightforward explanation for the above findings would be, apart from the characteristics of specific prion and mouse strains, that a minimum period of time is required for PrP^{Sc} to elicit neuronal impairment. On the other hand, the observation that PrP^C expression levels (rather than accumulation of PrP^{Sc}) correlate with the pace of clinical disease suggests that neuronal damage may be the consequence of the conversion of normal host prion protein (PrP^C) into PrP^{Sc}.

Corresponding Author:
Adriano Aguzzi, M.D.
Tel: +41 1 255 2107, Fax: +41 1 255 4402,
Email: adriano@pathol.unizh.ch

Δt infection-analysis (days)	Inoculum	Astrocytes/mm²	Neurons/mm²	Ratio astrocytes/ neurons	Astrocytes +neurons/mm²
98	Mock	168	764	4.55	932
98	Mock	372	892	2.40	1264
235	Mock	464	512	1.10	976
305	Mock	426	812	1.91	1238
305	Mock	616	568	0.92	1184
78	RML	1160	956	0.82	2116
78	RML	1068	552	0.52	1620
230	RML	2856	768	0.27	3624
285	RML	1124	324	0.29	1448
435	RML	4224	384	0.09	4608
425	RML	3080	200	0.06	3280

Table 1. Cell densities in neural grafts. Neurons and astrocytes were identified by morphological criteria and counted at various time points after mock inoculation (control grafts) or after infection with mouse prions. The left column indicates the latency between scrapie inoculation and histological analysis; the second column indicates the inoculum used (RML = Rocky Mountains Laboratory isolate). Third and fourth column indicate the density of astrocytes (or neurons respectively), calculated as cells per mm². The ratio between astrocyte and neuronal density is given in column five. In the right column, the overall cellular density is expressed in (neurons + astrocytes)/mm².

To clarify the pathogenetic importance of each of these events, we used the previously described neurografting paradigm (3, 16, 17) and transplanted embryonic neuroectoderm obtained from transgenic mice highly overexpressing PrP^C into recipient mice carrying a targeted deletion of the *Prnp* gene (6, 7). Since the latter are unsusceptible to scrapie, this setup allows for keeping scrapie-infected grafts viable in the context of a scrapie-resistant host (3) and enabled us to examine functional and histopathological alterations occurring during chronic scrapie disease. Of particular interest was the evaluation of the fate of neurons and astrocytes in scrapie-infected and degenerating grafts.

We also investigated the functionality of the blood-brain barrier (BBB) during disease progression by means of gadolinium-enhanced magnetic resonance imaging. BBB function relies on the interaction of astrocyte processes with CNS endothelium, and gliosis and BBB disturbances have been reported in experimental animal models (10) although the latter was never demonstrated unequivocally in humans (13, 29).

Materials and Methods

Animal strains and genotypes. Mice overexpressing the normal host prion protein (designated as $Prnp^{tga20/tga20}$) were generated by introducing multiple (30-50) copies of a *Prnp* transgene into $Prnp^{o/o}$ mice and breeding to homozygosity for the transgene (14). Thirty embryonal neuroectodermal grafts were derived from mating of homozygous $Prnp^{tga20/tga20}$ (table 1).

43 mice (strain 129SV x C57BL/6) carrying a homozygous disruption of the *Prnp* gene (7) were used as graft recipients. Disruption of the *Prnp* locus was confirmed by polymerase chain reaction genotyping (7). Female mice were kept in groups of 3-8 animals, while males were kept alone or in groups of up to three. All graft recipients were clinically monitored every second day for development of neurological deficits.

Neuroectodermal grafting procedure. Transplantation of neural tissue in mice was performed essentially as described (1, 3, 16, 18). Briefly, *tga20* transgenic mice overexpressing PrP^C were mated, and the morning at which a plug was detected was defined as E0.5. Embryos were harvested at day E12.5. Neuroectodermal tissue was dissected and implanted into the caudoputamen of anesthetized adult $Prnp^{0/0}$ mice using a stereotaxic frame and coordinates as described elsewhere (18).

Preparation of the infectious inoculum and inoculation procedure. Inoculation with mouse prions derived from the Chandler strain was performed according to published protocols (6). The RML2 (Rocky Mountains Laboratory) inoculum was prepared from brains of terminally sick CD-1 mice and a "mock inoculum", which was used in control experiments, consisted of homogenate analogously prepared from the brain of healthy CD1 mice.

We inoculated 27 grafted $Prnp^{o/o}$ mice intracerebrally with 30 μl of the scrapie prion inoculum two days, four weeks or eight weeks after the grafting procedure. For control experiments, nine grafted mice were inoculated with mock inoculum and another seven grafted mice did not receive any inoculum.

Magnetic resonance imaging. Magnetic resonance

imaging was performed on a 4.7T SISCO 200/330 NMR imaging spectrometer (Varian Int.). A 35 mm surface coil was positioned around the head of the animal, which was then placed in a plastic tube and was kept under inhalation anesthesia (1.2% isoflurane, 70% N_2O, 30% O_2). Data acquisition was performed with the following parameters: field of view 30x30mm, matrix size 256x256, 10 slices per animal, slice thickness 1mm, gap 1.2mm, number of excitations =4. Neural grafts were routinely visualized using T1 spin echo sequences (TE/TR= 18/260ms) and occasionally T2 (TR/TE= 55/3300ms) spin echo sequences. The condition of the blood-brain barrier was assessed by injection of 0.35 mmol/kg Gd-DTPA into the tail vein 10 min prior the scanning procedure. Scrapie-infected and healthy mice without grafts served as controls.

Histological and immunohistochemical examination. For paraffin histology, whole mouse brains were fixed for at least 24 h in 4% paraformaldehyde in phosphate buffered saline (PBS), immersed for 1h in 98% formic acid in order to reduce prion infectivity, and post-fixed for 72 h in 4% paraformaldehyde/PBS. Brains of control animals were treated identically. Coronal slices of approximately 2mm thickness were dehydrated through graded alcohols and embedded in paraffin. Sections of 4μm nominal thickness were mounted on TESPA (SIGMA Chemicals) coated glass slides and routinely stained with hematoxylin and eosin (H&E).

Grafts were considered for analysis if they had a minimum size of 100x200 μm and were detectable on at least ten serial sections. Grafts consisting of non-neural tissue, such as epithelium or cartilage, were excluded from analysis.

The age of the grafts of control group and test group was not attempted to match exactly, since we found earlier (3) that mock inoculated or uninoculated grafts show no differ-ences between day 70 and 430.

Immunohistochemistry for glial fibrillary acidic protein (GFAP, polyclonal, 1:300 (DAKO, Glostrup, DK)),) was performed on all paraffin embedded and frozen sections. In addition immunohistochemistry for synaptophysin (SY, polyclonal 1:40, DAKO), S100 (polyclonal 1:300 (DAKO)), and PrP (1B3, polyclonal 1:300 (12)) was performed on most of the sections (data not shown). On a subset of brains, in addition, immunostains for microglia (F4/80 polyclonal 1:400) was done (data not shown). Biotinylated secondary antibodies (goat-anti-rabbit; rabbit-anti-mouse, DAKO) were used at a dilution of 1:200. Visualization was achieved using biotin/avidin-peroxidase (DAKO) and diaminobenzidine as a chromogen following the protocols suggested by the manufacturer. Alternatively, brains were snap frozen in liquid nitrogen and stored at –80°C until cryosectioning for histoblot analysis (see below).

Histoblots. The histoblot technique has been employed according to published protocols (4, 26). Frozen sections of 12μm thickness were mounted on uncoated glass slides, immediately pressed on a nitrocellulose membrane wetted in lysis buffer and air-dried for at least 24 h. For detection, they were rehydrated in Tris buffered saline, and limited proteolysis was performed using proteinase K concentrations of 20, 50 and 100 μg/ml at 55°C for 8h. The sections were then denatured in 3M guanidinium thiocyanate for 10 min. and blocked for 1 h in 5% non fat milk serum. The primary antibody (anti-mouse PrP, 1B3, polyclonal 1:300 (12) was used at a dilution of 1:5000 in 1% non-fat milk overnight at 4°C. Detection was accomplished with an alkaline phosphatase conjugated goat-anti-rabbit antibody at a concentration of 1:2000. Visualization was achieved with nitroblue tetrazolium using 5-bromo-4-chloro-3-indolyl phosphate and 4-nitroblue tetrazolium chloride (Boehringer, Mannheim) according to the protocols of the supplier.

Morphometric analysis of the grafts. Cells were counted at high power magnification (20x objective) using a grid ocular. In all instances, all cells of the graft were counted and, after determination of the area covered by the graft, the total cellular density and that of astrocytes and of neurons were calculated and expressed as cells/mm^2. Astrocytes and neurons were distinguished upon their morphological appearance (Fig. 3) and astrocytes were additionally identified in GFAP immunostained sections. In some instances, two spatially segregated grafts were detected within one brain. In this case, both grafts were evaluated independently. Identical incubation time on the abscissa in Fig. 3 indicate that two grafts in one animal are evaluated independently. From the counted values, the standard error of mean was calculated (SEM= $\sqrt{1/n}$).

Results

Uninfected grafts overexpressing PrP develop normally. *Prnp*$^{tga20/tga20}$ grafts which had not been manipulated after the transplantation procedure (n=7), or which had been exposed to mock inoculum obtained from healthy CD-1 mice (n=9) served as controls and were used to define a base line for histological analysis.

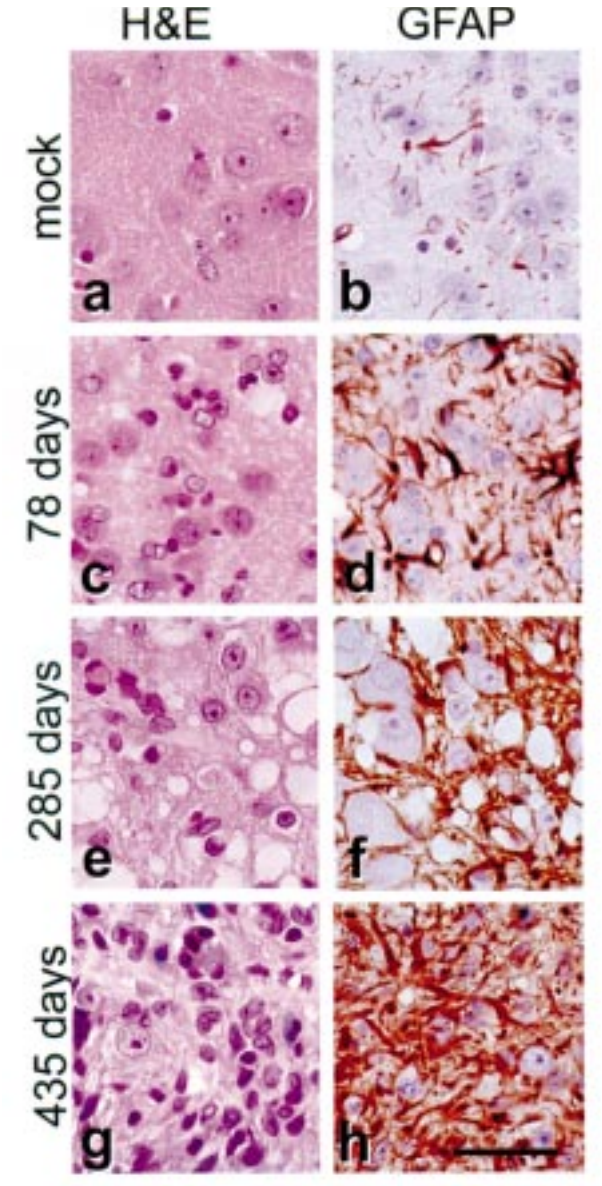

Figure 1. Histopathological analysis of neural *Prnp*$^{tga20/tga20}$ grafts. Upper row: mock-inoculated, 100 days after transplantation. 2. -4. row: 78, 285,and 435 days after RML-inoculation. Left column, hematoxylin & eosin stain; right column, immunohistochemistry for glial fibrillary acidic protein (GFAP).
a, b. typical appearance of an uninfected neural graft overexpressing PrP in a mock-infected *Prnp*$^{0/0}$ host brain. No spongiosis is present and the GFAP immunostain reveals only few astrocytes in the graft. **c, d.** 78 days after infection with scrapie: Dense, fine vacuolization, and brisk gliosis with occurrence of paired astrocytes. **e, f.** 285 days after scrapie infection: giant vacuolization and loss of neuronal processes. Astrocytes are wrapped around neurons and densely clustered. Overall cellular density is greatly increased at this time point but still apparently compensated by giant vacuoles. **g, h.** 450 days after infection, cellular density has increased considerably by (almost) total loss of neurons in the graft and by preservation of densely packed, small clustered astrocytes with thickened processes. Due to neuronal loss, only few small vacuoles are detected in such late stage grafts (scale bar =100 μm).

Figure 2. Opposite Page. Magnetic resonance imaging (MRI) and *post mortem* analysis of grafted mice: **a, b, c.** MRI examination 78 days after grafting and before inoculation. **d, e, f.** MRI 53 days and g, h,, i; 214 days after inoculation . Left (a, d, g) MRI before and after RML inoculation, before administration of gadolinium contrast medium. Middle (b, e, h), same animal after gadolinium contrast medium application. Right (c, f, i), contrast enhanced MRI of mock-infected control animal. No BBB leakage is detectable. *Post mortem* analysis of the respective brains: j, k, Histoblot analysis of the RML-inoculated grafted brain shows strong PrP-immunoreactivity in the area of the graft and the surrounding brain. Following proteinase K digestion (k) PrP^{Sc} accumulation in the graft and in the surrounding white matter is visualized. Histological analysis (m) of an adjacent frozen section (hematoxylin-eosin stain) confirms the presence of a graft in the right ventricle (scale bar =1mm). The area indicated by a box is shown at high power magnification in (m): Due to neuronal loss and astrogliosis, the graft became hypercellular (scale bar =100 μm). (l); Paraffin histology of the grafted, non-inoculated brain reveals a large, intraventricular graft. The area indicated by a box is shown at high power magnification in (l) stained with Luxol-Nissl (o) and immunostained with GFAP (p): The graft almost seamlessly integrated into the caudoputamen of the host and shows no spongiosis or gliosis.

Untreated and mock-infected grafts were analyzed between 72 and 478 days after the transplantation procedure and were indistinguishable by morphological appearance, size or by the extent of astrocytic reaction. Therefore, the age of the graft at the time point of analysis was not of crucial importance if scrapie prions were not administered. Uninfected grafts contained neurons, astrocytes (Fig. 1a, b) and oligodendrocytes (not shown) and occasionally showed mild gliosis, but never spongiosis or accumulation of proteinase resistant PrP.

Development of severe spongiform encephalopathy in infected neural grafts. First morphological changes characteristic for scrapie in grafts were detected 80 days after infection and progressively increased with time after infection. Thorough characterization of the events occurring during chronic scrapie is described in detail in (4) and will only be outlined here: 70-140 days after infection, brisk astrogliosis and spongiosis with small vacuoles is always encountered (Fig. 1c, d). With increasing incubation time of the grafts, astrogliosis becomes prominent, and giant vacuolization occurs at time points of 150-300 days after infection (Fig. 1e, f) but disappears at later stages (450 days, Fig. 1g, h).

Neuronal loss and increasing astrocyte density in

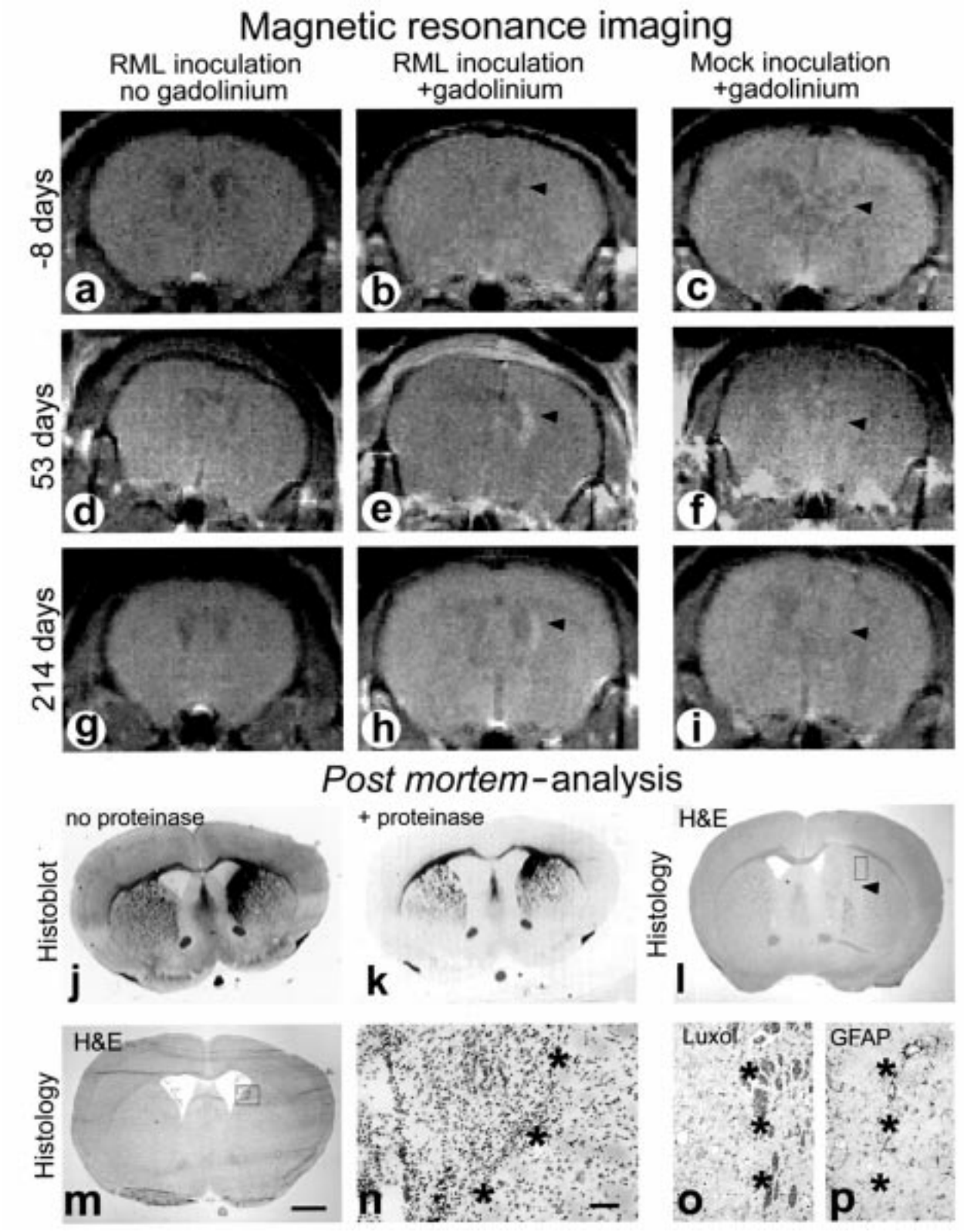
Magnetic resonance imaging
RML inoculation no gadolinium
RML inoculation +gadolinium
Mock inoculation +gadolinium
-8 days
53 days
214 days
a
b
c
d
e
f
g
h
i
Post mortem-analysis
no proteinase
+ proteinase
H&E
Histoblot
Histology
j
k
l
H&E
Luxol
GFAP
Histology
m
n
o
p

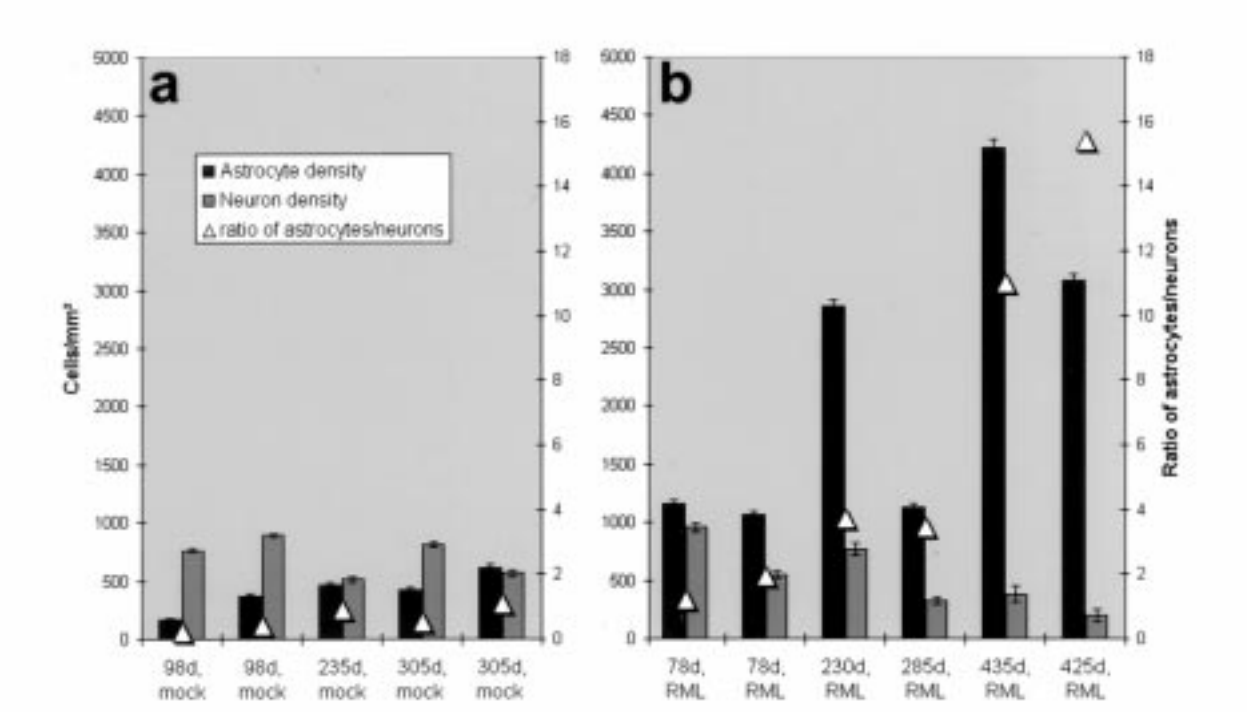

Figure 3. Cellular density in mock-infected and scrapie-infected grafts at different stages of the disease. Cellular density is expressed in cell count/mm² (left ordinate). To demonstrate the variability of the distribution of neurons and astrocytes in uninfected grafts, two spatially segregated grafts in individual animals were compared (98 and 305 days in mock-infected grafts and 78 days in RML-infected grafts). At 78 days after infection, a slight increase of astrocytic density can already be encountered, while significant neuronal loss is detected at later stages (285 days after infection). The ratio of neuronal to astrocytic density (triangles, values on the right ordinate) decreases already at earlier time points.

chronic scrapie disease. To define a baseline for the evaluation of cellular density and to detect neuronal loss after scrapie infection, neurons and astrocytes in 5 mock-infected grafts were counted upon morphological appearance and cellular density was calculated in cell count/mm. Therefore, variability in graft size did not influence the determination of cellular density. Neural grafts contained variable proportions of astrocytes, neurons and oligodendrocytes and showed variable spatial distributions of these components (Fig. 1a, b; Table 1; Fig. 3).

At *early* time points following scrapie infection (80 d, Fig. 1c, d; 3 animals), neuronal loss, as determined by neuronal density per mm² was inconspicuous, but significant gliosis was present, as reflected by the increased number of astrocytes/mm². At *intermediate* time points (140-280 days p.i., Fig. 1e, f; 8 animals), loss of neuronal processes and brisk astrocytic reaction with short, thickened processes wrapped around neurons was a prominent finding. Although this resulted in increased overall cellular density, the latter was partially counteracted by giant vacuolization. Therefore, actual neuronal loss may be more pronounced than indicated by the number of neurons/mm². *Late stage grafts* (280-480 days, Fig. 1g, h; 11 animals) were characterized by an almost complete loss of neurons. High cellularity was mainly due to strong predominance of densely packed astrocytes and to subtotal loss of neuropil as detected by loss of synaptophysin staining intensity and by the appearance of coarse perikaryal synaptophysin-positive granules detected upon immunostain (3). Spongiosis was much less prominent than at earlier time points, most likely because most cells which showed vacuolization in earlier stages had undergone degeneration.

In grafts of all histological stages as defined above, proteinase resistant protein was detected upon histoblot (data not shown). In a small subset of grafts there was some lymphocytic infiltration which may perhaps be ascribed to an occasional mild graft rejection. Generally, there were no lymphocytes detected. We performed microglia stains (F4/80) on a subset of grafts and found only relatively little amounts of microglia present even in aged grafts when compared to the strong astrocytic reaction. We have therefore not included these data into

our evaluation.

Breakdown of the blood-brain barrier during chronic scrapie infection. Blood-brain barrier reconstitution in non-infected neural grafts was assessed in 12 animals using gadolinium-enhanced magnetic resonance imaging at 69-86 days following the grafting procedure. In 11 of 12 animals, no leakage of contrast medium was observed, indicating that the BBB was functional (16), (Fig 2a, b, c). The single animal with incomplete reconstitution of the BBB was not included into the experimental group. Seven animals were subsequently inoculated intracerebrally with mouse prions, while four mice received mock inoculum intracerebrally and served as a control. All mice underwent subsequent imaging 53 or 54 days later and again 214, or 215 days after inoculation. As further controls, we analyzed scrapie-infected *tga20* mice (n=2) shortly before they developed clinical symptoms of scrapie and uninfected wild type mice (n=2).

In seven mice with a tight BBB within the neural graft, scrapie infection resulted in a persisting disruption of the BBB (Fig 2 d, e, g, h) while no BBB leakage was observed in mock infected grafted control mice (Fig. 2f, i). Examination of four grafted, mock-infected mice showed no disruption of the blood-brain barrier. Postmortem analysis of the inoculated brains with histoblots confirmed the presence of a graft with accumulation of proteinase resistant protein (Fig. 2 j, k), indicating that scrapie infection had taken place. Accumulation was detectable in grafts of all histological stages. Histological analysis of the grafted and mock-infected control brain showed large grafts in the left ventricle without signs of spongiform encephalopathy.

Discussion

Characterization of scrapie pathogenesis and progression in neuroectodermal grafts. Since scrapie-infected host mice do not develop clinical signs of scrapie disease (3), and the lifespan of an intracerebrally inoculated *tga*20 transgenic PrP overexpressing mouse ranges between 60 and 65 days (3, 14), inoculated grafts developing a spongiform encephalopathy were kept viable for a period of time corresponding to the sevenfold lifespan of an infected donor mouse. This model enabled us to study the chain of pathological events leading to neurodegeneration, and to determine the end point of the disease. Based on morphological criteria, the following events were detected: (i) development of spongiosis and gliosis (70 days); (ii) loss of neuronal processes within the grafts and subsequent destruction of the neuropil; (iii) increase of cellular density in the affected tissue (Fig. 3), probably due to astroglial proliferation; (iv) progression of the disease to complete loss of neurons (Fig. 1g, h); (v) reduction of the spongiosis in the terminal stage of the disease due to the loss of cells exhibiting vacuoles and, as previously described, accumulation of proteinase resistant protein.

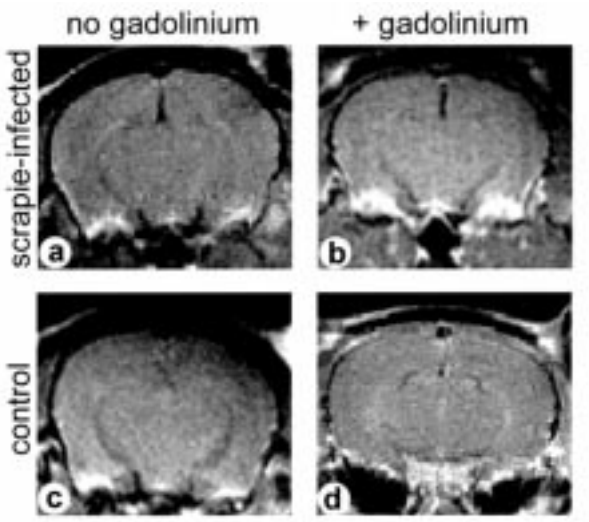

Figure 4. Magnetic resonance imaging of a scrapie-infected, terminally sick *tga20* mouse (a, b) and of a control mouse (c, d) prior to and following intravenous gadolinium administration. No significant differences of gadolinium enhancement between the scrapie-infected brain and the control brain are observed.

Following grafting, reconstitution of the BBB was confirmed by contrast enhanced MRI in 11 of 12 mice. Six mice with tight BBB were subsequently inoculated intracerebrally with mouse prions. This produced an obvious disruption of the blood-brain barrier within the graft already after 50 days, while no BBB leakage was detected in grafted and mock-inoculated control animals. BBB impairment in infected grafts persisted or progressed and existence of a degenerating scrapie-affected graft was confirmed by histoblot or histology.

In contrast to the above findings, *tga*20 mice with clinical symptoms of scrapie (60 days after intracerebral inoculation) showed no detectable BBB impairment in the brain (Fig. 4 a-d). On the other hand, it has been described that scrapie-infected hamsters with clinical symptoms of scrapie exhibit patchy BBB leakage upon gadolinium-enhanced MRI (10), while MRI studies of patients with Creutzfeldt-Jakob disease revealed increased signals in T2 weighted sequences but no significant BBB disruption (13, 19, 29). These discrepan-

cies could be ascribed to various factors: Since a functional BBB relies on intact astrocytic function and interaction of astrocytic processes with blood vessel endothelia (20, 27, 28), the observed leakage in the transplantation model may be due to astrocytic damage. Indeed, strong gliosis is attained in the grafts within 8-10 weeks after inoculation (Fig. 1 c, d). Hence, the absence of gadolinium leakage in terminally sick PrP overexpressing tga20 is in agreement with our observation that tga20 mice develop only a relatively mild astrogliosis at the end stage of the disease (S.B., Marek Fischer and A.A, unpublished results).

If the above assumptions were correct, by which mechanism would the BBB be impaired in spongiform encephalopathies? A straightforward explanation would be that scrapie affects the functional interaction of astrocytic endfeet with vessel endothelium. It is known that the latter interaction contributes to BBB function (20, 27, 28). Interestingly, this putative functional impairment does not lead to significant degeneration of astrocytes, which survive in large numbers until very late stages of disease in neural grafts. This is reflected by the persistence (and in some cases the progression) of BBB dysfunction in the grafting model during incubation time and is probably proportional to the extent of astrogliosis in the affected brain area (27). Further, our grafting model allows for disease progression to advanced stages of scrapie, which are not attained in other *in vivo* models: The very short latency between onset of clinical symptoms and death, in combination with a relatively mild gliosis might explain why BBB dysfunction is not detectable e.g. in *tga20* mice. In those models of scrapie in which gliosis is more prominent (e.g. hamster, and our grafting model), astrocyte dysfunction becomes prominent and is detectable as BBB leakage upon gadolinium enhanced MRI.

Although in some grafts we detected some scant lymphocytic infiltrates, autoreactive anti-PrP antibodies did not induce the observed pathological alterations of the BBB within the grafts. Such antibodies were indeed observed but similar titers were detected in grafted, non-infected, and in mock-infected mice which did not display any detectable abnormality when compared with $PrP^{0/0}$ mice grafted with $PrP^{0/0}$ tissue (2, 4).

Our findings confirm several predictions about the formal pathogenesis of spongiform encephalopathies: (i) scrapie leads to selective loss of neurons; (ii) astrocytes and perhaps other neuroectodermal cells, while being affected by the disease, can survive and maintain their phenotypic characteristics for very long periods of time and (iii) proteinase resistant protein accumulates in neuroectodermal tissue of all stages of the disease. It is unclear whether proteinase resistant PrP accumulates due to continued production by remaining cells (mainly astrocytes) or whether previously accumulated PrP is not cleared after PrP production ceased. Recent transgenetic studies (23) with mice expressing hamster-PrP^{C} under control of a GFAP promoter fragment have shown that astrocytes can support PrP^{Sc} accumulation, replication of the scrapie agent, and induction of the disease.

Disruption of BBB function is a finding that has been reported in experimental hamster scrapie (10) but was not found in human spongiform encephalopathies. The localized BBB disruption in chronically infected grafts may contribute to the spread of prions from grafts to the surrounding brain which was described previously (3). This would account for the accumulation of proteinase resistant PrP within the white matter and in brain areas surrounding the grafts. In view of the findings reported here, bulk-flow diffusion may be a mechanism contributing to prion spread as a consequence of prion-induced disruption of the blood-brain barrier.

Acknowledgments

We thank N. Wey for photographical artwork and M. König and B. Pfister for histological assistance. This study has been supported by the Kanton of Zürich and by grants from the Nationales Forschungsprogramm 38/38+, the European Union, the Bundesamt für Veterinärwesen (23-1477) and the Migros Foundation to A.A.

References

1. Aguzzi A, Blättler T, Klein MA, Räber A, Hegyi I, Frigg R, Brandner S, Weissmann C (1997) Tracking prions: The neurografting approach. *Cell. Mol. Life. Sci.* 53: 485-495
2. Blättler T, Brandner S, Raeber AJ, Klein MA, Voigtländer T, Weissmann C, Aguzzi A (1997) Transfer of scrapie infectivity from spleen to brain depends on interposed PrP-expressing tissue. *Nature* 389: 69-73
3. Brandner S, Isenmann S, Raeber A, Fischer M, Sailer A, Kobayashi Y, Marino S, Weissmann C, Aguzzi A (1996) Normal host prion protein necessary for scrapie-induced neurotoxicity. *Nature* 379: 339-43
4. Brandner S, Raeber A, Sailer A, Blaettler T, Fischer M, Weissmann C, Aguzzi A (1996) Normal host prion protein (PrPC) required for scrapie spread within the central nervous system. *Proc. Natl. Acad. Sci. USA* 93: 13148-13151
5. Büeler H, Raeber A, Sailer A, Fischer M, Aguzzi A, Weissmann C (1994) High prion and PrPSc levels but delayed onset of disease in scrapie-inoculated mice heterozygous for a disrupted PrP gene. *Mol Med* 1: 19-30
6. Büeler HR, Aguzzi A, Sailer A, Greiner RA, Autenried P, Aguet M, Weissmann C (1993) Mice devoid of PrP are resistant to scrapie. *Cell* 73: 1339-47

7. Büeler HR, Fischer M, Lang Y, Bluethmann H, Lipp HP, DeArmond SJ, Prusiner SB, Aguet M, Weissmann C (1992) Normal development and behaviour of mice lacking the neuronal cell-surface PrP protein. *Nature* 356: 577-582
8. Buyukmihci N, Goehring Harmon F, Marsh RF (1982) Optic nerve degeneration in hamsters experimentally infected with scrapie. *Exp Neurol* 78: 780-5
9. Buyukmihci N, Goehring Harmon F, Marsh RF (1982) Retinal degeneration during clinical scrapie encephalopathy in hamsters. *J Comp Neurol* 205: 153-60
10. Chung YL, Williams A, Beech JS, Williams SC, Bell JD, Cox IJ, Hope J (1995) MRI assessment of the blood-brain barrier in a hamster model of scrapie. *Neurodegeneration* 4: 203-7
11. DeArmond SJ, Prusiner SB (1997) Prion Diseases. In: Graham DI and Lantos PL (eds) Greenfield's Neuropathology. Arnold, London, vol 2, pp 235-271
12. Farquhar CF, Somerville RA, Ritchie LA (1989) Post-mortem immunodiagnosis of scrapie and bovine spongiform encephalopathy. *J Virol Methods* 24: 215-21
13. Finkenstaedt M, Szudra A, Zerr I, Poser S, Hise JH, Stoebner JM, Weber T (1996) Mr Imaging of Creutzfeldt-Jakob Disease. *Radiology* 199: 793-798
14. Fischer M, Rülicke T, Raeber A, Sailer A, Moser M, Oesch B, Brandner S, Aguzzi A, Weissmann C (1996) Prion protein (PrP) with amino-proximal deletions restoring susceptibility of PrP knockout mice to scrapie. *Embo J* 15: 1255-64
15. Giese A, Groschup MH, Hess B, Kretzschmar HA (1995) Neuronal cell death in scrapie-infected mice is due to apoptosis. *Brain Pathol* 5: 213-21
16. Isenmann S, Brandner S, Kuhne G, Boner J, Aguzzi A (1996) Comparative in vivo and pathological analysis of the blood-brain barrier in mouse telencephalic transplants. *Neuropathol Appl Neurobiol* 22: 118-28
17. Isenmann S, Brandner S, Sure U, Aguzzi A (1996) Telencephalic transplants in mice: characterization of growth and differentiation patterns. *Neuropathol Appl Neurobiol* 21: 108-117
18. Isenmann S, Molthagen M, Brandner S, Bartsch U, Kühne G, Magyar JP, Sure U, Schachner M, Aguzzi A (1995) The AMOG AMOG/b2 subunit of Na,K-ATPase is not necessary for long term survival of telencephalic grafts. *Glia:* 377-388
19. Ishida S, Sugino M, Koizumi N, Shinoda K, Ohsawa N, Ohta T, Kitamoto T, Tateishi J (1995) Serial MRI in early Creutzfeldt-Jacob disease with a point mutation of prion protein at codon 180. *Neuroradiology* 37: 531-4
20. Janzer RC, Raff MC (1987) Astrocytes induce blood-brain barrier properties in endothelial cells. *Nature* 325: 253-257
21. Jeffrey M, Fraser JR, Halliday WG, Fowler N, Goodsir CM, Brown DA (1995) Early unsuspected neuron and axon terminal loss in scrapie-infected mice revealed by morphometry and immunocytochemistry. *Neuropathol Appl Neurobiol* 21: 41-9
22. Masters CL, Richardson EP (1978) Subacute spongiform encephalopathy (Creutzfeldt-Jakob disease). The nature and progression of spongiform change. *Brain* 101: 333-344
23. Raeber AJ, Race RE, Brandner S, Priola SA, Sailer A, Bessen RA, Mucke L, Manson J, Aguzzi A, Oldstone MBA, Weissmann C, Chesebro B (1997) Astrocyte-specific expression of hamster prion protein (PrP) renders PrP knockout mice susceptible to hamster scrapie. *EMBO Journal* 16: 6057-65
24. Scott JR, Fraser H (1984) Degenerative hippocampal pathology in mice infected with scrapie. *Acta Neuropathol Berl* 65: 62-8
25. Scott JR, Jeffrey M, Halliday WG (1994) Unsuspected early neuronal loss in scrapie-infected mice revealed by morphometric analysis. *Ann N Y Acad Sci* 724: 338-43
26. Taraboulos A, Jendroska K, Serban D, Yang SL, DeArmond SJ, Prusiner SB (1992) Regional mapping of prion proteins in brain. *Proc Natl Acad Sci U S A* 89: 7620-4
27. Wisniewski HM, Lossinsky AS, Moretz RC, Vorbrodt AW, Lassmann H, Carp RI (1983) Increased blood-brain barrier permeability in scrapie-infected mice. *J Neuropathol Exp Neurol* 42: 615-26
28. Wolburg H, Neuhaus J, Kniesel U, Krauss B, Schmid EM, Ocalan M, Farrell C, Risau W (1994) Modulation of tight junction structure in blood-brain barrier endothelial cells. Effects of tissue culture, second messengers and cocultured astrocytes. *J.Cell Sci.* 107: 1347-1357
29. Yoon SS, Chan S, Chin S, Lee K, Goodman RR (1995) MRI of Creutzfeldt-Jakob disease: asymmetric high signal intensity of the basal ganglia. *Neurology* 45: 1932-3